

Autosomal Dominant Hypocalcemia Caused by a Novel Mutation in the Loop 2 Region of the Human Calcium Receptor Extracellular Domain

JIANXIN HU,¹ STEFANO MORA,² GIACOMO COLUSSI,^{3,4} MARIA CARLA PROVERBIO,²
KENDRA A. JONES,¹ LAURA BOLZONI,² MARIA E. DE FERRARI,³ GIOVANNI CIVATI,³
and ALLEN M. SPIEGEL¹

ABSTRACT

We report a novel missense mutation N124K in the extracellular calcium receptor (CaR) identified in two related subjects with the phenotypic features of autosomal dominant hypocalcemia (ADH). Expression of the N124K mutant receptor created by site-directed mutagenesis and transfected into HEK-293 cells was comparable with that of the wild-type (WT) receptor and two other mutant receptors N118K and L125P identified in subjects with ADH. Functional characterization by the extracellular Ca^{2+} ion ($[\text{Ca}^{2+}]_0$)-stimulated phosphoinositide (PI) hydrolysis in transfected HEK-293 cells showed that the N124K mutant receptor was left-shifted in Ca^{2+} sensitivity. This biochemical gain-of-function is comparable with that seen in other missense mutations of the CaR identified in subjects with ADH. We tested a series of missense substitutions (R, Q, E, and G) in addition to K for N¹²⁴ and found that only the N124K mutation and to a much lesser extent N124R caused a left shift in Ca^{2+} sensitivity. Thus, a specific substitution, not merely a mutation of the N¹²⁴ residue, is required for receptor activation. The N124K mutation is one of eight naturally occurring mutations in subjects with ADH identified in a short segment A¹¹⁶-C¹²⁹ of the CaR extracellular domain (ECD). We present a hypothesis to explain receptor activation by mutations in this region based on the recently described three-dimensional structure of the related metabotropic glutamate type 1 receptor (mGluR1). (*J Bone Miner Res* 2002;17:1461–1469)

Key words: autosomal dominant hypocalcemia, hypoparathyroidism, human calcium receptor, mutation, extracellular domain

INTRODUCTION

THE EXTRACELLULAR calcium receptor (CaR) is a G protein-coupled receptor (GPCR) that plays a key role in $[\text{Ca}^{2+}]_0$ homeostasis by regulating parathyroid hormone (PTH) secretion and renal Ca^{2+} reabsorption.^(1,2) Inactivat-

ing and activating mutations have been identified in the CaRs that are associated with familial hypocalciuric hypercalcemia and autosomal dominant hypocalcemia (ADH), respectively. With one exception, the A843E mutation that causes constitutive activation,^(3,4) naturally occurring mutations identified in subjects with ADH have been shown to cause an increase in sensitivity to $[\text{Ca}^{2+}]_0$ ("left-shift") rather than cause constitutive activation.^(1,2) We describe a

The authors have no conflict of interest.

¹Molecular Pathophysiology Section, National Institute on Deafness and Other Communication Disorders, National Institutes of Health, Bethesda, Maryland, USA.

²Laboratory of Pediatric Endocrinology, IRCCS H S. Raffaele, University of Milan, Milan, Italy.

³Renal Unit, Niguarda Ca' Granda Hospital, Milan, Italy.

⁴Present address: Renal Unit, Ospedale di Circolo e Fondazione Macchi, Varese, Italy.

novel CaR missense mutation N124K identified in a mother and daughter with the phenotypic features of ADH and show that this mutation, but not other substitutions for residue N¹²⁴, causes a substantially increased sensitivity to [Ca²⁺]_o. With N124K, a total of eight activating mutations have been identified in subjects with ADH in a short region A¹¹⁶-C¹²⁹ of the CaR extracellular domain (ECD).^(3,5-11) We present a possible explanation for mutational activation of the CaR by substitutions in this short region based on the recently described three-dimensional structure of the ECD of the related metabotropic glutamate type 1 receptor (mGluR1).⁽¹²⁾

MATERIALS AND METHODS

Patients

Two related women have been studied. The proband, a white woman, experienced generalized nocturnal seizures due to severe hypocalcemia when she was 42 years old. Inappropriately low levels of PTH were concomitantly present. A computed tomography (CT) scan performed during hospitalization disclosed bilateral basal ganglia calcifications. The patient was treated with oral calcium salts (1 g/day of elementary calcium) and calcitriol (0.7 µg/day). During treatment, her plasma calcium levels ranged from 1.95 to 2.12 mmol/liter (7.8–8.5 mg/dl; normal range, 2.12–2.55 mmol/liter or 8.6–10.2 mg/dl). Ten years later, she had a hypercalcemic crisis with dehydration, renal failure, hypotension, and paroxysmal atrial fibrillation. She was admitted at the Renal Unit, Niguarda Ca' Granda Hospital (Milan, Italy), and her plasma calcium was 3.74 mmol/liter (15 mg/dl) and plasma phosphorus was 1.77 mmol/liter (5.5 mg/dl; normal range, 0.87–1.42 mmol/liter or 2.7–4.4 mg/dl). During the last 6 years of follow-up, plasma calcium levels ranged from 1.95 to 2.25 mmol/liter (7.8–9 mg/dl), with urine calcium levels of 5.73–5.88 mmol/day (230–240 mg/24 h). PTH levels remained inappropriately low, compared with plasma calcium concentrations (7.1–37 pg/ml; normal range, 10–60 pg/ml).

The other patient is the second daughter of the proband. At 25 years of age, she experienced abrupt generalized seizures. Her ionized calcium levels were 0.76 mmol/liter (3.12 mg/dl). A CT scan disclosed faint basal ganglia calcification. During hospitalization, her plasma calcium levels were 2.0 mmol/liter (8.3 mg/dl), plasma phosphorus level was 1.48 mmol/liter (4.6 mg/dl). Intact serum PTH concentration was 30 pg/ml, and urinary calcium was 6.74 mmol/day (270 mg/24 h), with a calcium/creatinine ratio of 0.26 mg/mg.

Hypoparathyroid patients and healthy control subjects

Data from 18 patients with primary hypoparathyroidism were compared with data in ADH patients; 11 patients had postsurgical hypoparathyroidism, 5 patients had idiopathic hypoparathyroidism, and 2 patients had thalassemia with chronic transfusion-induced hemosiderosis. They were evaluated from once to up to 7 times, both off and on therapy for hypocalcemia, which included oral calcium

salts, vitamin D {usually 1,25-dihydroxyvitamin D₃ [1,25(OH)₂D₃], 0.25–1 µg/day}, aluminum-hydroxide (for the control of hyperphosphatemia), and a thiazide diuretic. Healthy control subjects ("controls") also were used for the analysis of P_{Ca}-PTH relationship; they were 13 subjects, whose data were already reported in another study.⁽¹³⁾ Individual calcium and PTH data were spontaneous random fasting values. Samples from all subjects were assayed using the same methods for calcium and PTH assay (N-tact PTH; Incstar Co., Stillwater, MN, USA). Informed consent was obtained for all studies.

DNA amplification and sequence analysis

Genomic DNA was isolated from white blood cells (Wizard, Genomic DNA Purification Kit; Promega, Madison, WI, USA), and the coding region of the CaR gene was polymerase chain reaction (PCR)-amplified using the primer pairs previously described.^(14,15) PCR was performed in a 100-µl reaction solution containing 400 ng of genomic DNA, 1.5 mmol of MgCl₂, 40 pmol of each primer, and 5 U of Eurobiotaq ADN Polymerase (Laboratoires EURO-BIO, Les Ulis Cedex, France). PCR products were purified using GFX PCR DNA and Gel Band Purification Kit (Amersham Pharmacia Biotech Italia, Milan, Italy).

Both manual and automatic sequencing were performed using the same primers used for PCR.

For manual sequence, the purified DNA fragments were sequenced by the Thermo Sequenase Radiolabeled Terminator Cycle Sequencing Kit (Amersham Pharmacia Biotech Italia) and reaction products were run on 6% polyacrylamide gel containing 8% urea and visualized by autoradiography.

Automatic sequencing was performed using fluorescence-labeled dideoxyterminators (Big Dye Terminator Cycle Sequencing Ready Reaction Kit, ABI PRISM; Applied Biosystems Foster City, CA, USA) according to the manufacturer's instructions and resolved by capillary electrophoresis on the ABI PRISM 310 Automated Sequencer (Applied Biosystems). Sequencing was performed in both strands.

Site-directed mutagenesis of the human CaR

The human CaR (hCaR) cDNA cloned in the pCR3.1 expression vector was described previously.⁽¹⁶⁾ Site-directed mutagenesis was performed using the Quickchange site-directed mutagenesis kit (Stratagene, Inc., La Jolla, CA, USA), according to the manufacturer's instructions. Parental hCaR cDNA in pCR3.1 vector was amplified using *pfu* Turbo DNA polymerase with mutagenic oligonucleotide primers (sequences available on request) for 16 cycles in a DNA thermal cycler (Perkin-Elmer, Norwalk, CT, USA). After digestion of the parental DNA with *DpnI* for 1 h, the amplified DNA with incorporated nucleotide substitution was transformed into *Escherichia coli* (DH-5α strain). The mutations were confirmed by automated DNA sequencing using a dRhodamine Terminator Cycle Sequencing kit and ABI PRISM-373A DNA sequencer (Applied Biosystems).

Transient transfection of wild-type and mutant receptors in HEK-293 cells

Transfections were performed using 12 μg (unless otherwise indicated) of plasmid DNA for each transfection in a 75-cm² flask of HEK-293 cells. DNA was diluted in serum-free DMEM (BioFluids, Inc., Rockville, MD, USA), mixed with diluted Lipofectamine (Gibco BRL, Grand Island, NY, USA) and the mixture was incubated at room temperature for 30 minutes. The DNA-Lipofectamine complex was diluted further in 6 ml of serum-free DMEM and was added to 80% confluent HEK-293 cells plated in 75-cm² flasks. After 5 h of incubation, 15 ml of complete DMEM containing 10% FBS (BioFluids, Inc.) was added. Twenty-four hours after transfection, transfected cells were split and cultured in complete DMEM.

Phosphoinositide hydrolysis assay

Phosphoinositide (PI) hydrolysis assay has been described previously.⁽¹⁶⁾ Briefly, 24 h after transfection, transfected cells from a confluent 75-cm² flask were split. Typically, one-eighth of cells were plated in one well in a 6-well plate and whole cell lysate was prepared 48 h posttransfection for Western blot assay. The remaining cells were plated in two 12-well plates in complete DMEM medium containing 3.0 $\mu\text{Ci/ml}$ of [³H]myoinositol (New England Nuclear, Beverly, MA, USA) and cultured for another 24 h. Culture medium was replaced by 1 \times PI buffer (120 mM of NaCl, 5 mM of KCl, 5.6 mM of glucose, 0.4 mM of MgCl₂, and 20 mM of LiCl in 25 mM of piperazine-*N,N*-bis[2-ethanesulfonic acid] (PIPES) buffer, pH 7.2) and incubated for 1 h at 37°C. After removal of PI buffer, cells were incubated for an additional 1 h with different concentrations of Ca²⁺ in 1 \times PI buffer. The reactions were terminated by addition of 1 ml of acid methanol (1:1000 vol/vol) per well. Total inositol phosphates were purified by chromatography on Dowex 1-X8 columns and radioactivity for each sample was counted with a liquid scintillation counter. Graphs of concentration dependence for stimulation of PI hydrolysis by [Ca²⁺]₀ for each transfection were drawn by using GraphPad Prism version 2.0 software (GraphPad Software, Inc., San Diego, CA, USA). Each value on a curve is the mean of duplicate determinations. Graphs shown in this study were representative ones from at least five independent experiments.

Immunoblotting analysis with detergent-solubilized whole cell extracts

Confluent cells in 6-well plates were rinsed with ice-PBS and scraped on ice in lysis buffer containing 20 mM of Tris-HCl (pH 6.8), 150 mM of NaCl, 10 mM of EDTA, 1 mM of EGTA, 1% Triton X-100, and freshly added protease inhibitors cocktail (Boehringer Mannheim, Indianapolis, IN, USA). The protein content in each sample was determined by the modified Bradford method (Bio-Rad Laboratories, Hercules, CA, USA) and 50 μg of protein per lane was separated on 5% SDS-PAGE gel under reducing conditions with 300 mM of β -mercaptoethanol added. The

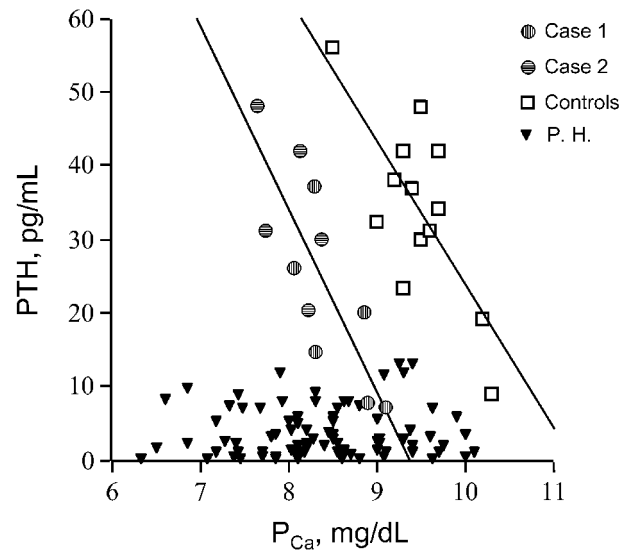


FIG. 1. The relationship between plasma calcium and PTH in ADH (hatched dots, case 1 and case 2), primary hypoparathyroidism (full triangles, P.H.), and in 13 healthy subjects (open squares, controls). Correlation lines are shown in ADH patients ($y = -25x + 233$; $p < 0.001$) and in control subjects ($y = -19x + 218$; $p < 0.001$).

proteins on the gel were electrotransferred onto a nitrocellulose membrane and incubated with 0.1 $\mu\text{g/ml}$ of protein A-purified mouse monoclonal anti-hCaR antibody ADD (raised against a synthetic peptide corresponding to residues 214–235 of hCaR protein). Subsequently, the membrane was incubated with a secondary goat anti-mouse antibody conjugated to horseradish peroxidase (Kirkegaard and Perry Laboratories, Gaithersburg, MD, USA) at a dilution of 1:5000. The hCaR protein was detected with an enhanced chemiluminescence system (ECL; Amersham Corp., Arlington Heights, IL, USA).

RESULTS

Relationship between plasma calcium and PTH

Over the range of plasma calcium values, there was a significant correlation between plasma calcium and PTH ($p < 0.001$) in patients with ADH but not in those with hypoparathyroidism (Fig. 1). The equation describing the relationship between plasma calcium and PTH in patients with ADH had a similar slope but different intercept from that in 13 healthy controls previously studied.⁽¹³⁾

Detection of a point mutation in the CaR gene

The sequence analysis of PCR-amplified genomic DNA revealed in both patients a heterozygous C to A transition at position 372 in exon 2 of the CaR gene (Fig. 2), causing a missense mutation N124K in the amino-terminal ECD of the receptor (Fig. 3).

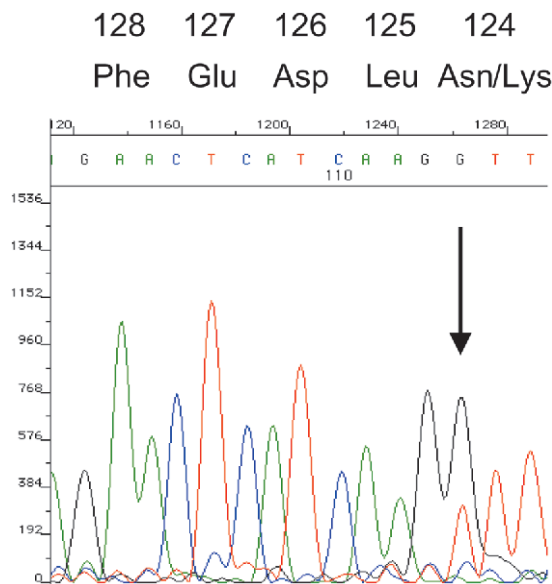


FIG. 2. Identification of the CaR mutation in a mother and daughter with ADH. Automated sequence analysis (reverse) of PCR-amplified genomic DNA from the affected subjects shows a heterozygous C to A transition at position 372 in exon 2 of the CaR gene, changing Asn to Lys.

Functional characterization of the N124K mutant hCaR

By site-directed mutagenesis, we constructed a mutant hCaR with N124K mutation using wild-type (WT) hCaR cDNA as a template. We transfected hCaR cDNA into HEK-293 cells and analyzed receptor expression on immunoblots stained with anti-hCaR monoclonal antibody ADD to detect total CaR immunoreactive species. We compared the N124K mutant CaR with WT and two other mutant CaRs N118K and L125P, which are adjacent to residue N¹²⁴. Both the N118K and the L125P mutations have been identified in subjects with ADH.^(3,6-8) Under reducing conditions, ADD antibody detected two major bands of ~130 kDa and 150 kDa at comparable expression levels for the WT hCaR and the three mutant hCaRs (Fig. 4). Previous studies have shown that the monomeric ~150-kDa band represents hCaR forms expressed at the cell surface and modified with N-linked, complex carbohydrates; the ~130-kDa band represents high mannose-modified forms, trapped intracellularly and sensitive to Endo-H digestion.^(9,16,17) We tested the function of the mutant receptor by using the intact cell $[Ca^{2+}]_0$ -stimulated PI hydrolysis assay. Figure 4 shows that HEK-293 cells transfected with vector only had no calcium response. The N124K mutant hCaR not only retained responsiveness to $[Ca^{2+}]_0$, but its Ca^{2+} sensitivity was increased also compared with WT hCaR. The effective concentration for 50% maximal response (EC_{50}) value for the N124K mutant hCaR was 1.58 ± 0.06 mM (mean \pm SE; $n = 5$) compared with a value of 3.08 ± 0.04 mM for the WT hCaR. EC_{50} values for N118K and L125P mutant hCaRs were 0.99 ± 0.05 mM and 0.71 ± 0.03 mM, respectively. Compared with the N118K and L125P mutant

hCaRs, the N124K mutant retains slightly greater expression seen on immunoblot (Fig. 4) and higher maximal calcium response. To determine if the increased sensitivity of the N124K mutant was caused by altered expression, we transfected cells with varying quantities of N124K mutant and WT hCaR cDNA and measured receptor expression by immunoblot and function by $[Ca^{2+}]_0$ -stimulated PI hydrolysis assay. Figure 5 shows that receptor expression increased with transfection of increasing amounts of DNA, but this affected maximal response to $[Ca^{2+}]_0$ and not EC_{50} values. Even when N124K mutant hCaR was expressed at a much lower level than the WT hCaR (compare 3 μ g of N124K vs. 12 μ g of WT hCaR DNA transfected), it still exhibited significantly increased sensitivity to $[Ca^{2+}]_0$ (Fig. 5).

Dominant effect of N124K mutation

The fact that the 2 patients we report here are heterozygotes with both WT and N124K mutant hCaR alleles suggests that the N124K mutation has a dominant effect in cells expressing both WT and N124K mutant hCaRs. Our in vitro study confirmed this. HEK-293 cells were cotransfected with equal amounts of WT and N124K mutant hCaR cDNA, and function was determined by $[Ca^{2+}]_0$ -stimulated PI hydrolysis assay. Figure 6 shows that sensitivity to $[Ca^{2+}]_0$ of cells transfected with equal amounts of N124K mutant and WT hCaR cDNA was intermediate between that of cells transfected with either the N124K mutant or the WT hCaR cDNA alone.

Comparison of function of mutant hCaRs with N¹²⁴ substituted by K, R, Q, E, or G

To determine if CaR activation is solely a function of substitution of N¹²⁴ or if activation depends on substitution of N¹²⁴ by specific amino acids, we constructed by site-directed mutagenesis four additional mutant hCaRs with residue N¹²⁴ replaced individually by R, Q, E, or G. Figure 7 shows the results of expression and functional assay of these mutants. Neither N124Q mutations (a conservative amino acid substitution) nor N124E (a replacement by an acidic residue) mutations affect the receptor's expression or function compared with the WT hCaR. The N124R mutation caused modest activation as evidenced by its response at 2 mM of $[Ca^{2+}]_0$, although its activating effect is much weaker than that of N124K, suggesting that a positive charge at residue 124 in hCaR by itself is insufficient to cause a substantial increase in sensitivity of the receptor to $[Ca^{2+}]_0$. Interestingly, N124G (a replacement by a neutral residue) shows a significant inactivating effect on the receptor. The N124G mutation also reduced the receptor's cell surface expression, further highlighting the unique functional consequences of substituting different amino acids for residue N¹²⁴.

DISCUSSION

Since the initial description of an activating hCaR mutation in a subject with ADH,⁽¹⁸⁾ a total of 26 mutations in the

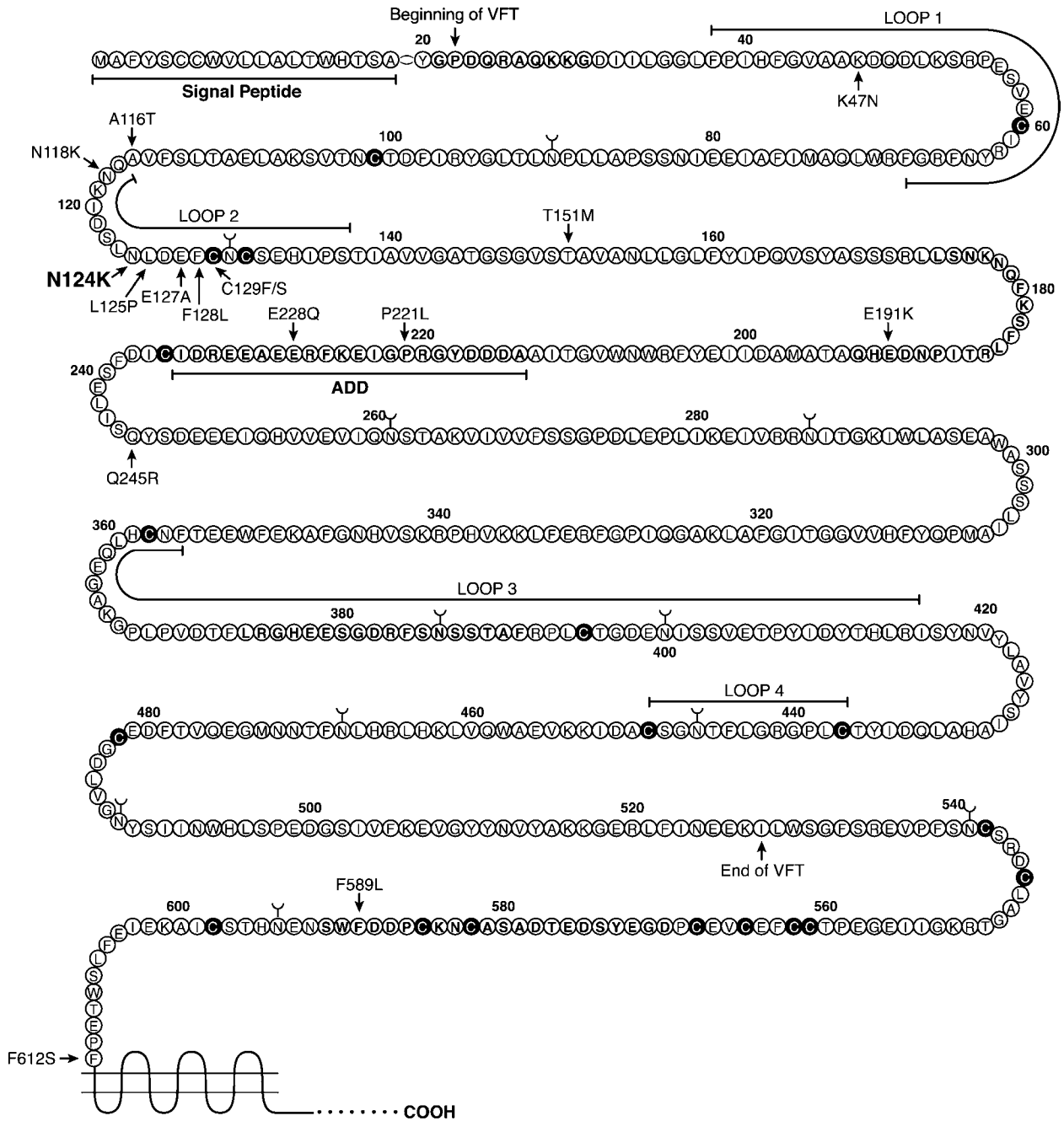


FIG. 3. Schematic diagram showing amino acid sequence of the hCaR ECD. The location of signal peptide, glycosylation sites, and the sequence of synthetic polypeptide used to raise monoclonal antibody ADD are indicated. All 19 cysteines are shown in black. The beginning and end of the VFT domain, and the four loops in lobe 1 of the VFT (see Discussion section) are indicated. Naturally occurring activating mutations identified in the ECD are indicated also.

hCaR have been reported in subjects with ADH.^(19,20) With the exception of a missense mutation A843E in the seventh transmembrane domain of the hCaR, which causes apparent constitutive receptor activation,^(3,4) functional characterization of other hCaR mutations identified in subjects with ADH has revealed an increase in Ca²⁺ sensitivity. Given that the receptor agonist ionized Ca²⁺ is always present at a finite concentration in the circulation, a mutation that in-

creases sensitivity to [Ca²⁺]₀ effectively can have the same consequence as gain-of-function mutations that can activate a given receptor in the absence of agonist. One might speculate that the degree of increase in sensitivity to [Ca²⁺]₀ caused by a particular hCaR mutation would correlate with the severity of the clinical phenotype. There is limited evidence supporting this suggestion. The A843E mutation that causes “true” constitutive activation and the L125P

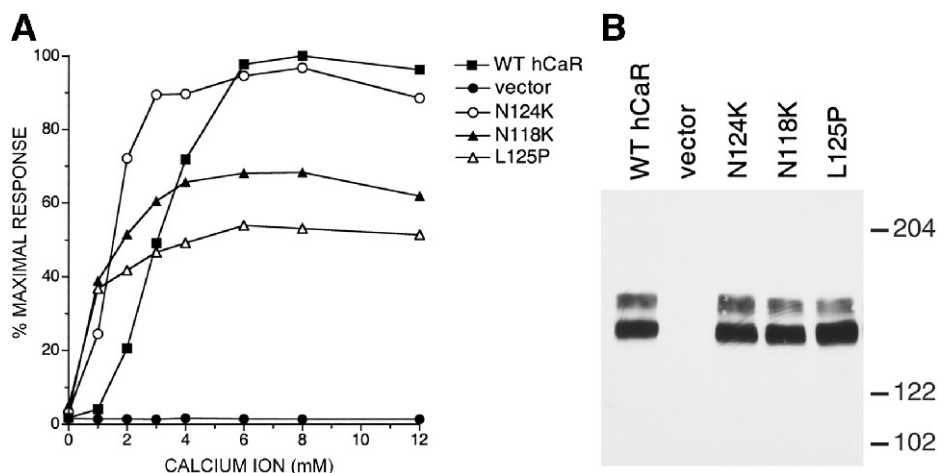


FIG. 4. (A) Concentration dependence for $[Ca^{2+}]_0$ stimulation of PI hydrolysis and (B) immunoblot of CaR in transiently transfected HEK-293 cells expressing WT hCaR, empty vector, N124K, N118K, and L125P mutant hCaRs. Transfection, PI assay, SDS-PAGE, and immunoblot with monoclonal anti-hCaR ADD were performed as described in the Materials and Methods section. Twelve micrograms of DNA each of the CaRs or empty vector was used in transfection. Molecular mass standards are indicated at the right of the blots. (A) Results of PI assay are expressed as percent of maximal response (WT hCaR at 8 mM). (B) Immunoblot of whole cell lysate of transfected HEK-293 cells. The immunoblots shown here and in Figs. 5–7 were done using cells from the same transfection as the cells used for the PI hydrolysis assay.

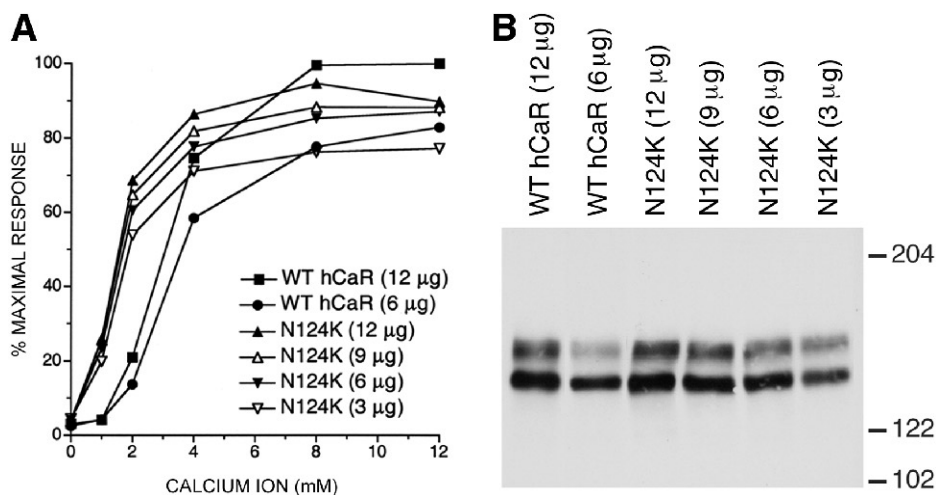


FIG. 5. (A) Concentration dependence for $[Ca^{2+}]_0$ stimulation of PI hydrolysis and (B) immunoblot of CaR (right) in transiently transfected HEK-293 cells expressing WT hCaR (12 µg and 6 µg of DNA transfected) and N124K mutant hCaR (12, 9, 6, and 3 µg of DNA transfected). Methods and format for presentation of results are as in legend to Fig. 4 except that maximal response is WT hCaR at 12 mM.

mutation that causes perhaps the most pronounced left shift in Ca^{2+} sensitivity, based on in vitro studies, were identified in subjects with particularly severe and early (age, <10 years) manifestations of hypocalcemia.⁽³⁾ In the present subjects, as in a number of previously reported cases of ADH,⁽¹⁹⁾ clinical manifestations were not apparent until adulthood. We found that the inverse relationship between plasma calcium and PTH is preserved in our subjects with ADH but that this relationship is shifted to the left by comparison with healthy control subjects.

We found that the N124K mutation caused a significant increase in CaR sensitivity to $[Ca^{2+}]_0$, but one that was less marked than either N118K or L125P mutations. In the mother and daughter reported here, hypocalcemia was first noted clinically at the ages of 42 years and 25 years, respectively. Although the age at diagnosis is consistent

with a less severe phenotype, it is likely that hypocalcemia had been present for a significant period before diagnosis, particularly because basal ganglion calcification was already present at the time of clinical diagnosis. Relative hypercalciuria, a specific feature of ADH reflecting the effect of CaR activation on renal reabsorption of $[Ca^{2+}]_0$, was of particular clinical significance in 1 of our subjects, leading to renal failure during attempted correction of hypocalcemia with calcium and calcitriol.

Of the total of 26 activating mutations identified in the hCaR in subjects with ADH, the majority (16 activation mutations) occur in the ECD (Fig. 3). The CaR is a member of family 3 of the GPCR superfamily.⁽²¹⁾ Members of family 3 are distinguished by having a particularly large amino-terminal ECD in addition to the seven transmembrane domain characteristic of the GPCR superfamily. The ECD

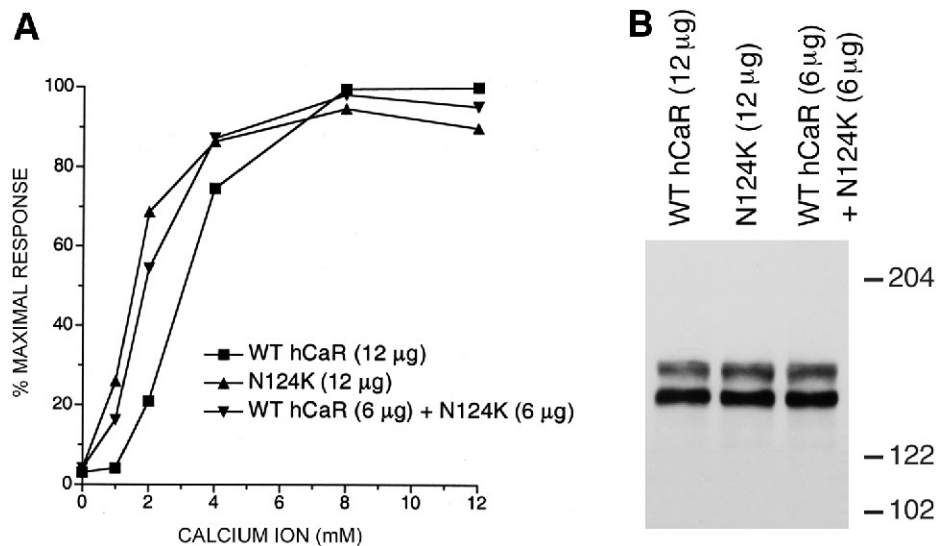


FIG. 6. (A) Concentration dependence for $[Ca^{2+}]_o$ stimulation of PI hydrolysis and (B) immunoblot of CaR in transiently transfected HEK-293 cells expressing WT hCaR (12 μg of DNA transfected), N124K mutant hCaR (12 μg of DNA transfected), and WT hCaR plus N124K mutant hCaR (6 μg of DNA each transfected). Methods and format for presentation of results are as in legend to Fig. 4 except that maximal response is WT hCaR at 12 mM.

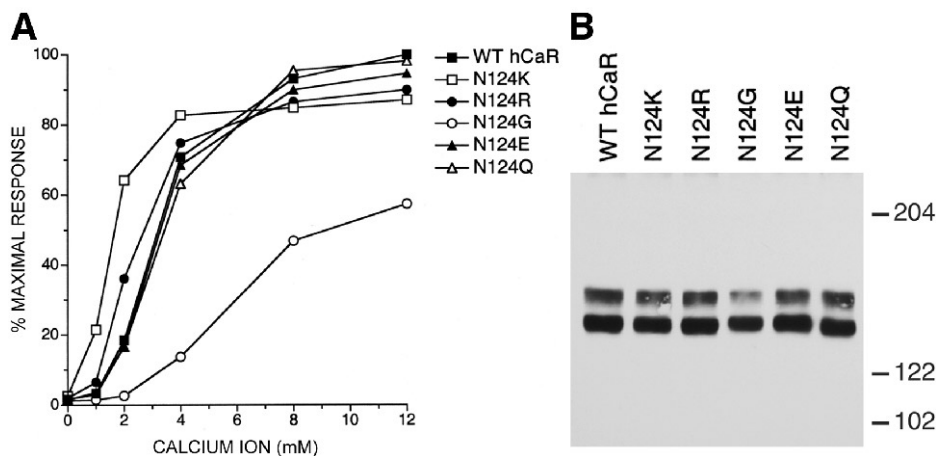


FIG. 7. (A) Concentration dependence for $[Ca^{2+}]_o$ stimulation of PI hydrolysis and (B) immunoblot of CaR in transiently transfected HEK-293 cells expressing WT hCaR, N124K, N124R, N124G, N124E, and N124Q mutant hCaRs. Methods and format for presentation of results are as in legend to Fig. 4 except that maximal response is WT hCaR at 12 mM. Twelve micrograms of DNA each of the CaRs was used in transfection.

of the CaR, the mGluRs and other members of family 3 consists of a Venus-flytrap (VFT) domain followed by a cysteine-rich domain that merges with the first transmembrane-spanning portion of the seven transmembrane domain.⁽²²⁻²⁴⁾ The VFT domain is so named because, as first shown for the bacterial periplasmic binding proteins,⁽²⁵⁾ it consists of two “lobes” that are open in the unliganded state and that close on ligand binding. Recently, the three-dimensional structure of a portion of the ECD (lacking the cysteine-rich domain) of the rat mGluR1 in both the unliganded and the glutamate-bound conformations was determined by X-ray crystallography.⁽¹²⁾ The structure was that of a bilobed VFT that was open in the unliganded form and closed with glutamate-bound form. Based on the three-dimensional structure of the mGluR1 VFT domain, a schematic diagram of both the free form (without binding of Ca^{2+}) and the complex form (with binding of Ca^{2+}) of the dimeric hCaR VFT domains is shown in Fig. 8. One lobe of the VFT (the amino-terminal lobe we have termed “lobe 1”) shows four loops of varying length (Fig. 3 shows the sequence and length of each of these loops) protruding from

the lobe itself.⁽²²⁾ Of these loops, loop 2 is of particular significance and is depicted in Fig. 8. We had shown earlier that cysteines 129 and 131 within loop 2 of the hCaR are involved in intermolecular disulfide bonds that are the basis for covalent dimerization of the CaR ECD.⁽²²⁾ Homologous cysteines are involved in intermolecular disulfide-linked dimers in other family 3 members including mGluRs.

Comparison of the three-dimensional structures of the open versus closed conformations of the mGluR1 VFT shows an $\sim 70^\circ$ rotation about an axis through the VFT dimer interface (Fig. 8). Loop 2 is involved not only in covalent disulfide-linked dimerization, but it also forms a portion of the dimer interface. Thus, it is particularly interesting that of 16 activating mutations in the hCaR ECD, 8 including the presently reported N124K mutant occur in the proximal portion of loop 2 between residues A¹¹⁶ and C¹²⁹. A saturation mutagenesis study of the A¹¹⁶-P¹³⁶ region of the hCaR also showed that mutation of this region frequently leads to receptor activation.⁽²⁶⁾ Unfortunately, the structure of the majority of loop 2 was indistinct in the mGluR1 crystal structure, but in the amino-terminal portion

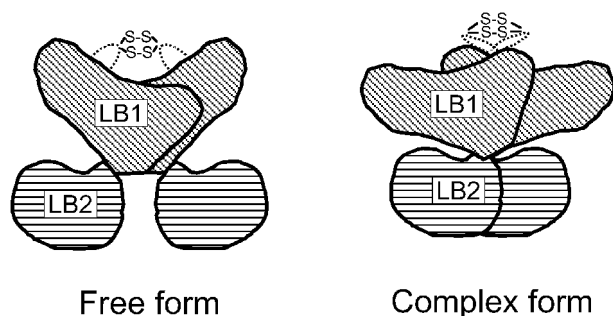


FIG. 8. Diagram of free (no ligand bound) and complex (agonist-bound; agonist not shown in diagram) forms of the dimeric hCaR VFT domains. Lobe 1 (LB 1) and lobe 2 (LB 2) of the VFT domain of one monomer are labeled. The loop 2 region of lobe 1 is shown as a dotted line with residues C¹²⁹ and C¹³¹ involved in intermolecular disulfide linkage.

of loop 2 there was a notable difference observed between the open and closed conformations.⁽¹²⁾ In the former, an α -helix forming a portion of the dimer interface was extended for several residues into loop 2. In the glutamate-bound, closed conformation, this α -helical extension was not present.

The clustering of activating mutations in loop 2 of the hCaR leads us to propose the following mechanism for CaR activation by such mutations, based on the crystal structure of the related mGluR1 VFT. Without Ca²⁺ bound to it, the CaR VFT dimer remains in the open position (Fig. 8, free form). Ca²⁺ binding promotes closing of the VFT that is accompanied by a significant rotation of one VFT monomer relative to the other (Fig. 8, complex form). This rotation involves a change in structure in at least the proximal portion of loop 2 from an α -helix to a more disordered loop. We suggest that activating mutations in loop 2 change its structure and thereby decrease the normal constraints to rotation of the VFT dimer. This would have the effect of facilitating VFT closure at any given Ca²⁺ concentration, hence increasing sensitivity of the receptor to activation by Ca²⁺. Such a mechanism is consistent with our previous results⁽²²⁾ showing that mutations of cysteines 129 and 131 that prevent covalent (but not noncovalent) dimerization do not abolish CaR response but rather increase sensitivity to Ca²⁺. However, not every mutation in loop 2 results in CaR activation as seen with the various substitutions at N¹²⁴ that either caused no change or in the case of N124G actually reduced receptor expression and activation. Ultimately, determination of the structure of the CaR VFT in unliganded and Ca²⁺-bound conformations, including loop 2 in native and mutated form, will be necessary to validate this hypothesis. Nonetheless, further identification and study of naturally occurring activating mutations such as those clustered in loop 2, as well as those in other locations, should offer unique insights into the structure and function of the CaR.

ACKNOWLEDGMENTS

We are grateful to Stephen Marx for careful reading of this paper. L. Bolzoni was supported by a Fellowship from Pharmacia & Upjohn Italy.

REFERENCES

1. Brown EM, MacLeod RJ 2001 Extracellular calcium sensing and extracellular calcium signaling. *Physiol Rev* **18**:239–297.
2. Brown EM 2000 G protein-coupled, extracellular Ca²⁺ (Ca₀²⁺)-sensing receptor enables Ca₀²⁺ to function as a versatile extracellular first messenger. *Cell Biochem Biophys* **33**:63–95.
3. Nakae J, Shinohara N, Tanahashi Y, Murashita M, Abe S, Hasegawa T, Hasegawa Y, Fujieda K 1997 New mutations of Ca²⁺-sensing receptor gene in two Japanese patients with sporadic hypoparathyroidism with hypercalciuria. *Horm Res* **48**(Suppl 2):179.
4. Zhao XM, Hauache O, Goldsmith PK, Collins R, Spiegel AM 1999 A missense mutation in the seventh transmembrane domain constitutively activates the human Ca²⁺ receptor. *FEBS Lett* **448**:180–184.
5. Baron J, Winer KK, Yanovski JA, Cunningham AW, Laue L, Zimmerman D, Cutler GB Jr 1996 Mutations in the Ca²⁺-sensing receptor gene cause autosomal dominant and sporadic hypoparathyroidism. *Hum Mol Genet* **5**:601–606.
6. Pearce SH, Williamson C, Kifor O, Bai M, Coulthard MG, Davies M, Lewis-Barned N, McCredie D, Powell H, Kendall-Taylor P, Brown EM, Thakker RV 1996 A familial syndrome of hypocalcemia with hypercalciuria due to mutations in the calcium-sensing receptor. *N Engl J Med* **335**:1115–1122.
7. De Luca F, Ray K, Mancilla EE, Fan GF, Winer KK, Gore P, Spiegel AM, Baron J 1997 Sporadic hypoparathyroidism caused by de novo gain-of-function mutations of the Ca²⁺-sensing receptor. *J Clin Endocrinol Metab* **82**:2710–2715.
8. Hauache OM, Hu J, Ray K, Xie R, Jacobson KA, Spiegel AM 2000 Effects of a calcimimetic compound and naturally activating mutations on the human Ca²⁺ receptor and on Ca²⁺ receptor/metabotropic glutamate chimeric receptors. *Endocrinology* **141**:4156–4163.
9. Bai M, Quinn S, Trivedi S, Kifor O, Pearce SHS, Pollak MR, Krapcho K, Hebert SC, Brown EM 1996 Expression and characterization of inactivating and activating mutations in the human Ca₀²⁺-sensing receptor. *J Biol Chem* **271**:19537–19545.
10. Lienhardt A, Bruckert E, Turpin G, Bai M, Kottler ML 2000 New mutation of the calcium-sensing receptor. The 82nd Annual Meeting of The Endocrine Society, Toronto, Canada, June 21–24, 2000 (abstract 1720).
11. Hirai H, Nakajima S, Miyauchi A, Nishimura K, Shimizu N, Shima M, Michigami T, Ozono K, Okada S 2001 A novel activating mutation (C129S) in the calcium-sensing receptor gene in a Japanese family with autosomal dominant hypocalcemia. *J Hum Genet* **46**:41–44.
12. Kunishima N, Shimada Y, Tsuji Y, Sato T, Yamamoto M, Kumasaka T, Nakanishi S, Jingami H, Morikawa K 2000 Structural basis of glutamate recognition by a dimeric metabotropic glutamate receptor. *Nature* **407**:971–977.
13. Colussi G, Macaluso M, Brunati C, Minetti L 1994 Calcium metabolism and calciotropic hormone levels in Gitelman's syndrome. *Miner Electrolyte Metab* **20**:294–301.
14. Pearce SHS, Trump D, Wooding C, Besser GM, Chew SL, Grant DB, Heath DA, Hughes IA, Paterson CR, Whyte MP, Thakker RV 1995 Calcium-sensing receptor mutations in familial benign hypercalcemia and neonatal hyperparathyroidism. *J Clin Invest* **96**:2683–2692.
15. Ho C, Conner DA, Pollak MR, Ladd DJ, Kifor O, Warren HB, Brown EM, Seidman JG, Seidman CE 1995 A mouse model of human hypocalciuric hypercalcemia and neonatal severe hyperparathyroidism. *Nat Genet* **11**:389–394.
16. Ray K, Fan GF, Goldsmith PK, Spiegel AM 1997 The carboxyl terminus of the human calcium receptor: Requirements for cell-surface expression and signal transduction. *J Biol Chem* **272**:31355–31361.

17. Ray K, Clapp P, Goldsmith PK, Spiegel AM 1998 Identification of the sites of N-linked glycosylation on the human calcium receptor and assessment of their role in cell surface expression and signal transduction. *J Biol Chem* **273**:34558–34567.
18. Pollak MR, Brown EM, Estep HL, McLaine PN, Kifor O, Park J, Hebert SC, Seidman CE, Seidman JG 1994 Autosomal dominant hypocalcaemia caused by Ca^{2+} -sensing receptor gene mutation. *Nat Genet* **8**:303–307.
19. Hendy GN, D'Souza-Li L, Yang B, Canaff L, Cole DEC 2000 Mutations of the calcium-sensing receptor (CASR) in familial hypocalciuric hypercalcemia, neonatal severe hyperparathyroidism, and autosomal dominant hypocalcemia. *Hum Mutat* **16**:281–296.
20. Hauache OM 2001 Extracellular calcium-sensing receptor: Structural and functional features and association with diseases. *Braz J Med Biol Res* **34**:577–584.
21. Bockaert J, Pin JP 1999 Molecular tinkering of G protein-coupled receptors: An evolutionary success. *EMBO J* **18**:1723–1729.
22. Ray K, Hauschild BC, Steinbach PJ, Goldsmith PK, Hauache O, Spiegel AM 1999 Identification of the cysteine residues in the amino-terminal extracellular domain of the human Ca^{2+} receptor critical for dimerization: Implications for function of monomeric Ca^{2+} receptor. *J Biol Chem* **274**:27642–27650.
23. Hu J, Hauache O, Spiegel AM 2000 Human Ca^{2+} receptor cysteine-rich domain: analysis of function of mutant and chimeric receptors. *J Biol Chem* **275**:16382–16389.
24. Hu J, Reyes-Cruz G, Goldsmith PK, Spiegel AM 2001 The Venus's-flytrap and cysteine-rich domains of the human Ca^{2+} receptor are not linked by disulfide bonds *J Biol Chem* **276**:6901–6904.
25. O'Hara PJ, Sheppard PO, Thogersen H, Venezia D, Haldeman BA, McGrane V, Houamed KM, Thomsen C, Gilbert TL, Mulvihill ER 1993 The ligand-binding domain in metabotropic glutamate receptors is related to bacterial periplasmic binding proteins. *Neuron* **11**:41–52.
26. Jensen AA, Spalding TA, Burstein ES, Sheppard PO, O'Hara PJ, Brann MR, Krogsgaard-Larsen P, Brauner-Osborne H 2000 Functional importance of the Ala 116-Pro 136 region in the calcium-sensing receptor. *J Biol Chem* **275**:29547–29555.

Address reprint requests to:
Jianxin Hu, Ph.D.
Building 10, Room 8C-101
National Institutes of Health
9000 Rockville Pike
Bethesda, MD 20892, USA

Received in original form October 16, 2001; in revised form January 24, 2002; accepted March 8, 2002.